

# Immobilization studies of *Candida Antarctica* lipase B on gallic acid resin-grafted magnetic iron oxide nanoparticles

This article was published in the following Dove Press journal:  
*International Journal of Nanomedicine*

Nagaraja SreeHarsha<sup>1</sup>  
Ravindra V Ghorpade<sup>2</sup>  
Abdullah Mossa Alzahrani<sup>3</sup>  
Bandar E Al-Dhubiab<sup>1</sup>  
Katharigatta N Venugopala<sup>1,4</sup>

<sup>1</sup>Department of Pharmaceutical Sciences, College of Clinical Pharmacy, King Faisal University, Al-Ahsa, Saudi Arabia;

<sup>2</sup>Chemical Engineering and Process Development Division, CSIR-National Chemical Laboratory, Pune 411 008, India; <sup>3</sup>Department of Biological Sciences, College of Science, King Faisal University, Al-Ahsa, Saudi Arabia; <sup>4</sup>Department of Biotechnology and Food Technology, Durban University of Technology, Durban 4001, South Africa

**Purpose:** Here, we present the successful preparation of a highly efficient gallic acid resin grafted with magnetic nanoparticles (MNPs) and containing a branched brush polymeric shell.

**Methods:** Using a convenient co-precipitation method, we prepared Fe<sub>3</sub>O<sub>4</sub> nanoparticles stabilized by citric acid. These nanoparticles underwent further silica modification and amino functionalization followed by gallic acid functionalization on their surface. Under alkaline conditions, we used a condensation reaction that combined formaldehyde and gallic, to graft the gallic acid–formaldehyde resin on the surface. We then evaluated the polymer-grafted MNPs to assay the *Candida Antarctica* B lipase (Cal-B) immobilization via physical adsorption.

**Conclusion:** Furthermore, during optimization of parameters that defined conditions of immobilization, we found that the optimum immobilization was achieved in 15 mins. Also, optimal immobilization temperature and pH were 38°C and 7.5, respectively. In addition, the reusability study of immobilized lipase polymer-grafted MNPs was done by isolating the MNPs from the reaction medium using magnetic separation, which showed that grafted MNPs reached 5 cycles with 91% activity retention.

**Keywords:** nanoparticles, *Candida Antarctica* lipase B, *grafting*, *immobilization*

## Introduction

*Candida Antarctica* lipase B (Cal-B) is an enzyme with numerous applications in a broad range of catalytic reactions and is often used in industrial chemical processes<sup>1–4</sup> such as kinetic resolutions, aminolysis, esterification, transesterification, hydrolysis, and stereoisomeric transformations<sup>3,5–8</sup> and even the synthesis of glucolipids.<sup>9,10</sup> Cal-B is highly selective, offering stability in an acidic pH environment, as high-quality end-product, and with fewer side-products from chemical reactions. It is also highly effective at high temperatures.<sup>11</sup>

Uppenberget al<sup>12</sup> were the first to elucidate the structure of Cal-B. It is comprised of 317 amino acids and weighs ~33 kDa. The structure reveals a conserved core that is eight-stranded with a twisted β-sheet sandwiched by α-helices on both sides.<sup>12,13</sup> The active site contains a serine. However, the sequences around the active serine site are different in Cal-B as compared to other lipases. Cal-B contains the foundation for the Ser-His-Asp/Glu residues that form the catalytic triad. The surface that surrounds the tip of the active site is hydrophobic, and this allows for interaction with lipid surfaces in hydrolysis. During hydrolysis, the surface has aliphatic residues that form side chains which are oriented toward the solvent.<sup>12</sup>

Correspondence: Nagaraja SreeHarsha  
Department of Pharmaceutical Sciences,  
College of Clinical Pharmacy, King Faisal  
University, Al-Ahsa, Saudi Arabia  
Tel +96 653 548 5322  
Email sharsha@kfu.edu.sa

Despite the unique and excellent features of Cal-B in biotransformation, these properties are absent once they are dissolved in organic solvents. They are also easily denatured when subjected to high temperatures, mechanical shear, and various solvent effects.<sup>14</sup> It is also difficult to recover the enzyme from reaction solutions or separate it from both substrates and products. Altogether, these factors underlie the major reasons for the seldom use of biocatalysts in the pharmaceutical industry. Proteins, more especially enzymes, are amphipathic, which makes them intrinsically active at their surface and lends them to be highly absorptive.<sup>15</sup> Adsorption-driven immobilization is due to enzyme binding to a solid support.<sup>16</sup>

One way to improve enzyme performance is to change their bound state through either ionic forces, physical adsorption, hydrophobic bonds, and Van der Waals forces or combination of all these forces.<sup>17</sup> Theoretically, it is possible to develop catalysts that portray significant advantages relative to free enzyme using the technique of enzyme immobilization.<sup>18–20</sup> Previous work using this method has demonstrated remarkable improvements in performance including increased enzyme activity (up to a factor of 100) in organic solvents, increased enantioselectivity, remarkable long-term stability, increased temperature stability, and more efficient recovery by filtration or centrifugation.<sup>17–19</sup> Consistent with this, many studies report the effective use of immobilized Cal-B in transformation reactions for compounds with low molecular mass<sup>21,22</sup> and reactions involving polymerization.<sup>23,24</sup> However, adsorption induces conformational changes that affect catalyst rate and specificity.<sup>25</sup> As a result, research on immobilization has focused on matrix selection and the optimization of conditions.<sup>26–29</sup>

Enzyme immobilization offers the advantage of efficiently increasing enzyme yield and recovery. This method offers a wider range of possibilities such as enzyme reuse in other types of reactions, and increasing enzyme stability and activity. Furthermore, postreaction, these enzymes also demonstrate a higher temperature resistance and are more tolerant to organic solvents.<sup>30,31</sup>

Gallotannins are a subclass of plant tannins that are hydrolyzable. These compounds have recently received a growing amount of attention due to the excellent characteristics that make them suitable for use as adhesives in place of phenolic compound derived from petroleum. The hydrolysis of these compounds produces gallic acid, an aromatic ring with a carboxyl group, and three adjacent hydroxyl groups.<sup>32</sup> Previous work has demonstrated that

polymer-coated nanoparticles have more magnetic susceptibility and a larger polymer surface area for enzyme immobilization.<sup>33</sup> Furthermore, lipases that are immobilized using a magnetic support can be removed from a reaction system and stabilized using a bed reactor that has been fluidized with an external magnetic field.<sup>34,35</sup> Last, using magnets as a support reduces the cost of operations and total capital.<sup>36,37</sup>

In this study, we demonstrate a facile, bio-inspired approach to immobilizing Cal-B enzyme onto poly(gallic acid–formaldehyde)-modified magnetic nanoparticles (MNPs). Polyphenolics demonstrate better adhesive performance due to the phenolic hydroxyl groups they possess.<sup>38</sup> The phenolic moieties present in gallic acid are reactive to nucleophiles such as primary amines, making them capable of immobilizing Cal-B enzyme. To test this idea, we functionalized magnetic silica nanoparticles with amino groups and modified them with gallic acid. Under alkaline conditions, we carried out a condensation reaction between gallic acid and formaldehyde to prepare a resin graft of gallic acid–formaldehyde onto magnetic silica nanoparticles. We then used the obtained nanoparticles as an adsorbent for enzyme Cal B.

Our results demonstrate that poly(gallic acid–formaldehyde)-modified MNPs exhibit high efficiency for enzyme Cal-B immobilization. Even after many cycles of magnetic separation and reuse, we found that the enzyme retained a

high degree of activity. We observed maximal Cal-B lipase binding and expression by optimizing the parameters of immobilization by changing the time of immobilization and loading of enzymes. Finally, we evaluated how stable the lipases were in their free and immobilized states by measuring the storage, pH, and temperature.

## Experimental section

### Materials

We purchased ferric chloride hexahydrate (97%), gallic acid (99%), formaldehyde solution (37% in water), 3-aminopropyltrimethoxysilane (APTMS, 97%) and tetraethylorthosilicate (99%) from Sigma Aldrich (St Louis, MO, USA). Potassium bromide (IR grade) was purchased from Merck (India). Ethyl acetate (GC grade) and ferrous chloride hydrate (98%) were purchased from Loba Chemie (India). Cal-B was commercially obtained from Fermenta Biotech Ltd. (India). All chemicals were reagent grade and purchased from local suppliers.

## Synthesis of amino-functionalized MNPs ( $\text{Fe}_3\text{O}_4@\text{SiO}_2@\text{APTMS}$ )

We prepared MNPs via the co-precipitation of iron (II) and iron (III) chloride under basic conditions. This process was stabilized by the chemical adsorption of citric acid on the surface. We modified the Stober method<sup>39</sup> and used silica to coat nanoparticles of magnetic particles using a basic mixture of ethanol and water set at 30°C and magnetic fluids for seeding. We then ensured that the amino groups were anchored to magnetic silica particles using the reaction of magnetic  $\text{SiO}_2$  with APTMS to obtain  $\text{Fe}_3\text{O}_4@\text{SiO}_2@\text{NH}_2$ .<sup>40</sup>

## Gallic acid-modified MNPs ( $\text{Fe}_3\text{O}_4@\text{SiO}_2@\text{GA}$ )

We dispersed 3.0 g of a functionalized form of amino MNPs ( $\text{Fe}_3\text{O}_4@\text{SiO}_2@\text{APTMS}$ ) in 40 mL of 1,4-dioxane using sonication. A solution was made by dissolving 3.0 g of gallic acid in 20 mL of 1,4 dioxane, and 0.2 g of boric acid was added to this solution. A solution of gallic acid–boric acid was added to the nanoparticle dispersion while stirring at 800 rpm in a 250 mL glass reactor. The reaction mixture was kept stirring at 80°C for 10 hrs under nitrogen. Subsequently, the flask was cooled and the products ( $\text{Fe}_3\text{O}_4@\text{SiO}_2@\text{GA}$ ) were separated using magnets and intensely sonicated using water and acetone. The product was then dried using a vacuum at room temperature.

## Gallic acid–formaldehyde resin-grafted MNPs ( $\text{Fe}_3\text{O}_4@\text{SiO}_2@\text{PGA}$ )

3.0 g of gallic acid-grafted MNPs ( $\text{Fe}_3\text{O}_4@\text{SiO}_2@\text{PGA}$ ) was dispersed in 80 mL of deionized water and then ultrasonicated for 20 mins. This suspension was kept stirring at 800 rpm, while the reaction was heated and maintained to 65°C. 12.0 g of gallic acid was added to the nanoparticle suspension with the successive addition of 57 mL of formaldehyde solution. Afterward, 40 mL of ammonia solution was added while maintaining the temperature at 85°C. This reaction mixture was kept stirring for 3 hrs. After cooling, the reaction mixture was acidified with 1 N  $\text{HNO}_3$ .  $\text{Fe}_3\text{O}_4@\text{SiO}_2@\text{PGA}$  nanoparticles were separated and rinsed with  $\text{H}_2\text{O}$  DMF followed by ethanol. Last, the final product was vacuum dried at room temperature.

## Characterization of MNPs

- (a) Transmission electron microscopy (TEM): we employed this technique to examine the surface morphology and internal structure of MNPs. Specimens

were prepared by first mounting the MNPs on a copper grid with a 200-mesh carbon coating. We then placed 20  $\mu\text{L}$  of the liquid sample containing nanoparticles on a grid of copper and left it to dry overnight at room temperature. Micrographs were then taken on a JEOL 1200-EX instrument with the voltage accelerated at 100 kV.

- (b) X-ray diffraction (XRD) analysis: we used a Rigaku X-ray diffractometer to examine the crystalline phase of the polymer-grafted MNPs.
- (c) FTIR spectroscopy: to examine the extent of infrared absorption, a Shimadzu 8300-Fourier transform infrared spectrophotometer with a resolution of  $1\text{ cm}^{-1}$  in the transmission mode was used. We milled 3 mg of the polymer and mixed it with 100 mg potassium bromide. We pressed this into a 12 mm diameter solid disk prior to the measurement of FTIR.
- (d) Thermogravimetric analysis (TGA). We examined the thermal stability and grafting amount of the nanoparticle using TGA (STA 6000). Samples were heated starting from 30°C to 900°C temperature at a rate of  $10^\circ\text{C min}^{-1}$  under conditions of dry nitrogen.
- (e) Magnetic behavior of MNPs: we used the Lakeshore (Model 7407) vibrating-sample magnetometer (VSM) to determine the magnetization curves of the dried nanoparticles. We applied a magnetic field that ranged in strength from  $-15,000$  to  $15,000$  Oe at 30°C.

## Immobilization of Cal-B on $\text{Fe}_3\text{O}_4@\text{SiO}_2@\text{PGA}$

50 mg of  $\text{Fe}_3\text{O}_4@\text{SiO}_2@\text{PGA}$  nanoparticles was placed in 2 mL capped vials (centrifuge tubes). 0.5 mL of DMSO was sonicated for a minute and kept for 6 hrs for the polymer to swell. After 6 hrs, DMSO was separated from the rest of the mixture using centrifugation. Subsequently, a solution of Cal-B (0.7 mL, 7 mg/mL) and a buffer of sodium phosphate (0.7 mL, pH 7.5) were added to MNPs. The reaction mixture was thoroughly mixed to ensure that the MNPs encountered soluble Cal-B. This mixture was kept for 15 hrs for the immobilization of Cal-B. After 15 hrs, the solution was separated by centrifugation. The resulting immobilized Cal-B enzyme was washed twice with a buffer of sodium phosphate (0.35 mL, pH 7.5). Both supernatant and washing solution were collected and assayed using ethyl acetate as the

substrate, with 0.1 N NaOH for an estimation of the protein levels. The difference between the enzyme that was loaded and unbound enzyme indicated the amount of immobilized enzyme on the MNPs. The enzyme activity for both soluble and immobilized enzyme was calculated based on hydrolysis of ethyl acetate and expressed as EAU per unit weight.

## Enzymatic assay

The immobilized enzyme was added to a beaker that contained 13 mL of distilled water, 2.5 mL of a buffer of sodium phosphate (100 mM, pH 7.5), and 1 mL of ethyl acetate and incubated for 5 mins at room temperature, and then constantly stirred. The reaction was halted using 3 mL acetone solution. The activity of the immobilized enzyme was further determined with the titrimetric method using 0.1 N NaOH and 1% phenolphthalein as an indicator for ethyl acetate. The reaction was titrated to the end-point, using the pink color change for phenolphthalein as the indicator.

## Results and discussion

To synthesize functionalized magnetic silica nanoparticles of gallic acid ( $\text{Fe}_3\text{O}_4@\text{SiO}_2@\text{GA}$ ), we first prepared iron oxide nanoparticles by the co-precipitation of Fe(II) and Fe(III). Next, we sought to improve the affinity of  $\text{Fe}_3\text{O}_4$  nanoparticles to target species, which was accomplished by introducing reactive silanol groups on the surface of  $\text{Fe}_3\text{O}_4$  using tetraethyl orthosilicate (TEOS). The TEOS-modified  $\text{Fe}_3\text{O}_4$  nanoparticles were subsequently treated with APTMS. This treatment with APTMS allowed the nanoparticles to covalently bind to the free  $-\text{OH}$  groups at the surface of the particles, while the amino group at the end could couple with the carboxylic acid group in gallic acid. This final step of the reaction allowed for the formation of the gallic acid-functionalized magnetic silica nanoparticles ( $\text{Fe}_3\text{O}_4@\text{SiO}_2@\text{GA}$ ). The resultant MNPs were then treated with gallic acid and formaldehyde solution under alkaline conditions to yield a gallic acid–formaldehyde resin grafted with MNPs ( $\text{Fe}_3\text{O}_4@\text{SiO}_2@\text{PGA}$ ). The polymer-grafted MNPs were then exposed to a lipase-containing solution to achieve enzyme immobilization (Figure 1).

To observe and analyze the degree of surface modifications and polymer grafting of the nanoparticles, we carried out an FTIR spectrum of the MNPs (Figure 2). In examining the FTIR spectrum of the MNPs only, we observed a broad stretching vibrational peak at  $3,474\text{ cm}^{-1}$ . The spectrum includes O-H bonds attached to iron atoms. We also observed an absorption at  $587\text{ cm}^{-1}$  that are Fe-O bonds. The silica

coating of the iron oxide nanoparticles portrayed several Si-O vibration bands around  $1,082\text{ cm}^{-1}$ . We also observed stretches of alkyl C-H at  $2,975$  and  $2,930\text{ cm}^{-1}$  and primary amines that showed N-H bending at  $1,555\text{ cm}^{-1}$  in the APTMS-functionalized MNPs, as compared to that of silica-coated MNPs. Furthermore, we observed additional aromatic C-H stretching vibrations at  $3,100\text{ cm}^{-1}$ , which confirmed the covalent bonding of gallic acid on MNPs. Using the FTIR peak analysis, the polymerization of gallic acid–formaldehyde was confirmed on the surface of  $\text{Fe}_3\text{O}_4@\text{SiO}_2@\text{GA}$ .

We also obtained TEM images of magnetic uncoated iron oxide and polymer-grafted silica core/shell MNPs as shown in Figure 3A and B. We observed that the size of the  $\text{Fe}_3\text{O}_4$  nanoparticles ranged from 15 to 20 nm. In Figure 3B, we demonstrate that core MNPs were covered with silica coating and polymer grafting. During the process, we observed aggregation of some MNPs. In sum, a silica shell followed by polymer grafting seemed to be formed around the nanoparticles.

We used XRD to examine the crystalline structure of the MNPs that were polymer grafted. This method revealed that the diffraction pattern of MNPs is consistent with a previously reported structure of crystalline silica-coated MNPs (Figure 4).<sup>41,42</sup> As shown in the figure, peak characteristic for  $\text{Fe}_3\text{O}_4$  indicated by their indices (220), (311), (400) and (511), and (440) were examined for polymer-grafted nanoparticles and showed that the resulting nanoparticles were  $\text{Fe}_3\text{O}_4$  alone with an inverse structure.<sup>41</sup> The amorphous nature of grafted polymer accounts for the initial broad peak.

To quantify the amount of modification and polymer grafting on the magnetic  $\text{Fe}_3\text{O}_4$  nanoparticles, we carried out a TGA, as demonstrated in Figure 5. We observed a minor weight loss in the MNPs in the temperature range of  $100^\circ\text{C}$ , which we attributed to the remaining  $\text{H}_2\text{O}$ . Our data demonstrate that the % weight of polymer grafted on MNPs is 40.

We measured GA-MN's magnetic moment measured using the sample's magnetometry, with a magnetic strength in the range of  $-15,000\text{ Oe}$  to  $15,000\text{ Oe}$ . We show a plot of  $M$  vs  $H$ , at room temperature in Figure 6. Our data showed that the saturation magnetization ( $M_s$ ) value of enzyme bounded polymer-grafted MNPs was  $21\text{ emu/g}$ . We found this to be lower in value as compared to the  $M_s$  value ( $65\text{ emu/g}$ ), which is exhibited by the unmodified iron oxide MNPs. The reduction in MNPs' magnetic moment is because of an equal amount of nonmagnetic coating and the polymer grafting. We validated this

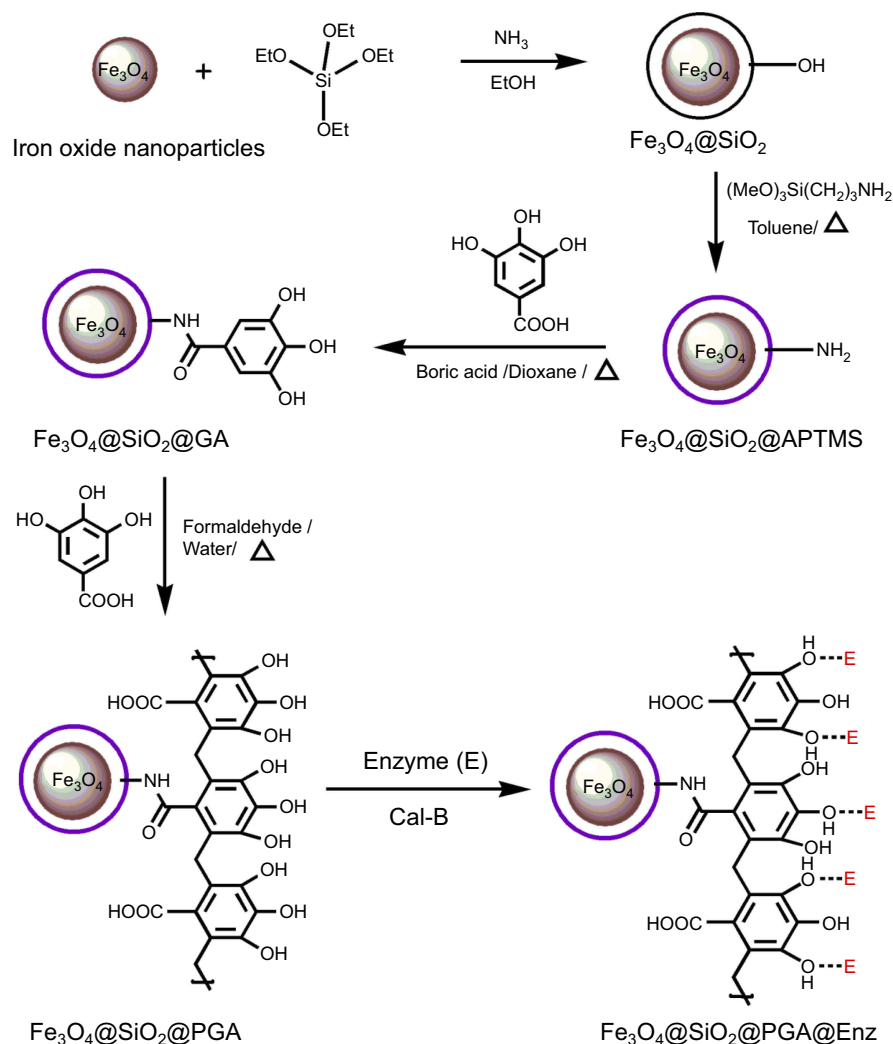


**Figure 1** Schematic diagram for the preparation route of Cal-B enzyme immobilized polymer-grafted magnetic silica nanoparticles.

combination using the TGA. Regardless, we found the magnetization value to be adequate for enzyme removal of loaded MNPs after the reaction was completed. We believed this to be due to the high sensitivity of the MNPs to the external magnet. In Figure 7, we demonstrate the successful separation of enzyme-loaded polymer of grafted nanoparticles from the reaction mixture using an external magnetic field.

## Optimization of immobilization time

In Figure 8, we demonstrate the results of experiments to determine the optimal time needed for the immobilization of the lipase (gallic acid–formaldehyde)-grafted MNPs (Figure 8). Our results show that the EAU activity of Cal-B immobilized MNPs reached equilibrium in

15 h. However, after that, the enzymatic activity of the MNPs that were immobilized was found to be constant.

## Optimization of enzyme loading

To determine optimal enzyme loading conditions, we determined the effect of adding various quantities of enzyme to the portion of the enzyme that was immobilized. Our results demonstrated that increasing the amount of the loaded enzyme directly increased the initial enzyme concentration. However, that quickly reached a maximum value. To further evaluate the loading capacity, the polymer-grafted MNPs were loaded with different concentrations of the Cal-B enzyme and examined for their levels of protein binding and lipase activity. Results are listed in Table 1. We observed a direct correlation between the activity of immobilized enzyme and an increase in enzyme loading concentration,



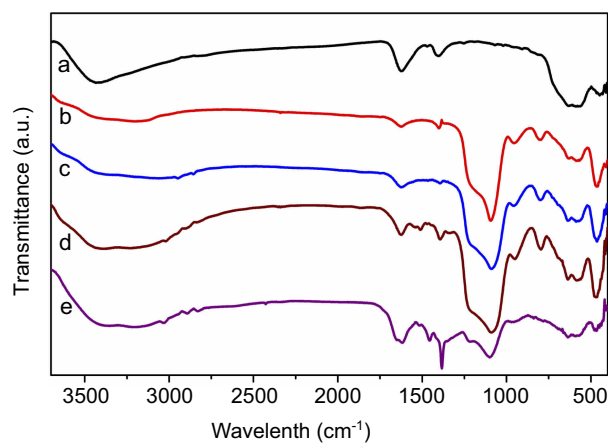


**Figure 2** FTIR spectra of (a)  $\text{Fe}_3\text{O}_4$  MNPs, (b) silica-coated MNPs, (c) amino-functionalized MNPs, (d) gallic acid-modified MNPs, (e) gallic acid-formaldehyde resin-grafted MNPs.

at 15,000 EAU/g. However, the opposite was the case as the activity decreased when concentrations  $>15,000$  EAU/g were used. Therefore, our results demonstrate that the Cal-B molecules are immobilized proximal to each other, thereby preventing any deactivation caused by the unfolding of the enzyme, and hindering the support surface.<sup>16,43</sup> Also, lack of increase of activity with increase of nominal amount in contact with the support could be assigned to the aggregation of CALB in polar solvent.<sup>44</sup>

### Effect of pH value on immobilized lipase activity

We also carried out a comparative study of the pH between free and immobilized Cal-B enzyme on polymer-grafted nanoparticles. The variation in the comparative activity of both free and immobilized Cal-B enzyme at varied pH values is showcased in Figure 9A. Our results demonstrate that the best pH values were 7.0

and 7.5 for the immobilizes and free enzyme, respectively. The free lipase had an optimum pH that was shifted by 0.5 units to alkaline pH values after immobilization. Our results show that the immobilized enzyme on polymer-grafted MNPs demonstrates adaptability in a wide region of pH values compared to the free lipase. The method of immobilization, structure, and charge of the matrix determines the observed difference and shift. We contend that our results are due to the extent of stabilized lipase molecules due to the multipoint immobilization on the polymer-grafted MNPs.

### Effect of temperature on immobilized lipase activity

The restricted conformational mobility of lipase following immobilization often occurs due to deactivation forces. As such, we investigated the effect of temperature on lipase molecules that were either immobilized or free, and where we used ethyl acetate as a substrate (Figure 9B). The optimum temperature of nonimmobilized or free lipase appeared at  $27^\circ\text{C}$ , but the lipase that was immobilized was obtained at  $38^\circ\text{C}$ , which is much higher than the free lipase. Interestingly, immobilized lipase was still activated at temperatures above  $38^\circ\text{C}$ . As the temperature increased, the relative activity of immobilized lipase degreed to a less degree as compared to that of free lipase. Immobilized lipase demonstrated an optimum temperature that was up to  $38^\circ\text{C}$ , and higher than its soluble version. Furthermore, we observed resistance to high temperatures in the immobilized lipase.

Repeated enzyme use in experiments and industrial applications is perhaps the most important benefit of enzyme immobilization. We carried out a set of experiments on catalyst reusability to determine the stability of

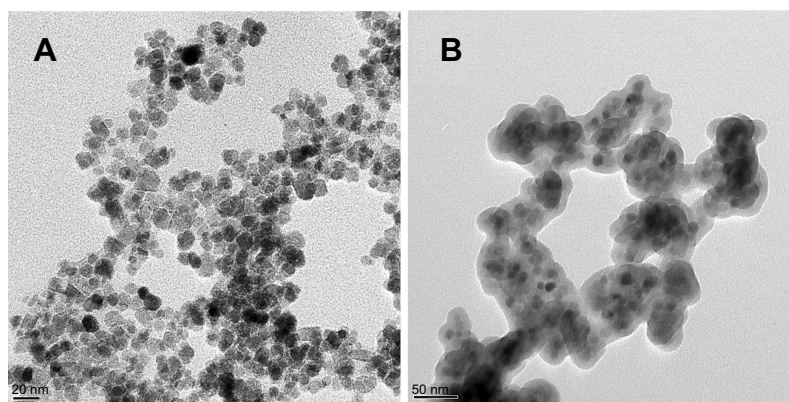


**Figure 3** TEM images of (A)  $\text{Fe}_3\text{O}_4$  nanoparticles and (B)  $\text{Fe}_3\text{O}_4@SiO_2@PGA$  magnetic silica nanoparticles.

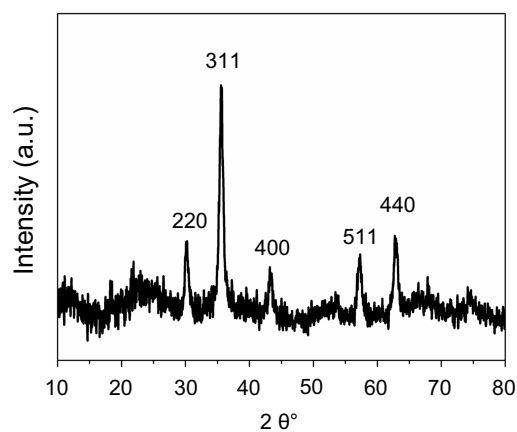


**Figure 4** X-ray diffraction (XRD) spectra of the polymer-grafted magnetic silica nanoparticles.

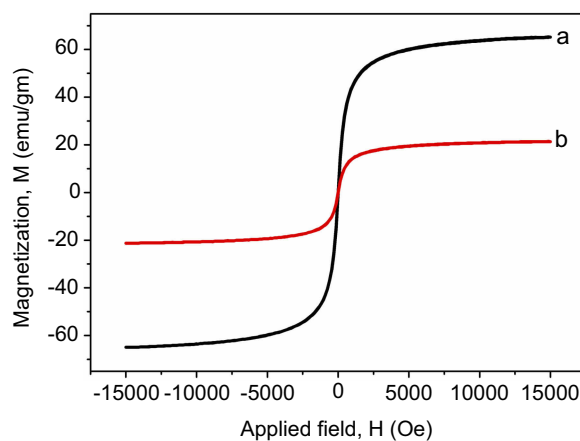


**Figure 6** The magnetic hysteresis loops of (a) neat iron oxide and (b) polymer-grafted iron oxide MNPs.

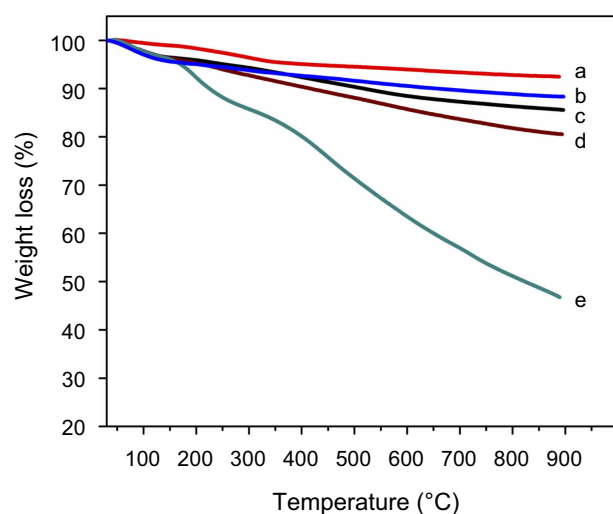


**Figure 5** TGA thermograms of (a)  $\text{Fe}_3\text{O}_4$  nanoparticles, (b) silica-coated magnetic nanoparticles, (c) amino-functionalized magnetic nanoparticles, (d) gallic acid-modified magnetic nanoparticles, (e) gallic acid-formaldehyde resin-grafted magnetic nanoparticles.

immobilized enzyme. After seven cycles, immobilized lipase activity was significantly decreased as shown in

Figure 10. Nonetheless, we still observed a baseline level of stability, as activity remained at 91% even after the first five cycles. After the completion of five cycles, the activity of immobilized Cal-B decreased drastically. As such, it can be concluded that during the initial round of adsorption, the enzyme is neither deactivated nor denatured. Observed decreases in activity may result from extrinsic factors such as leakage of enzymes, desorption of residual lipase that was strongly adsorbed, and configuration changes.

## Conclusion

We demonstrate that a gallic acid resin grafted with magnetic iron oxide nanoparticles provides significant support for Cal-B enzyme immobilization. Synthesized polymer-grafted MNPs were thoroughly characterized to understand their structure. The gallic acid resin-grafted MNPs displayed a high lipase loading capacity due to its core-shell nanostructure and strong adhesive interactions between the enzyme and grafted polymer. Indeed, the immobilized Cal-B enzyme on gallic acid resin-grafted

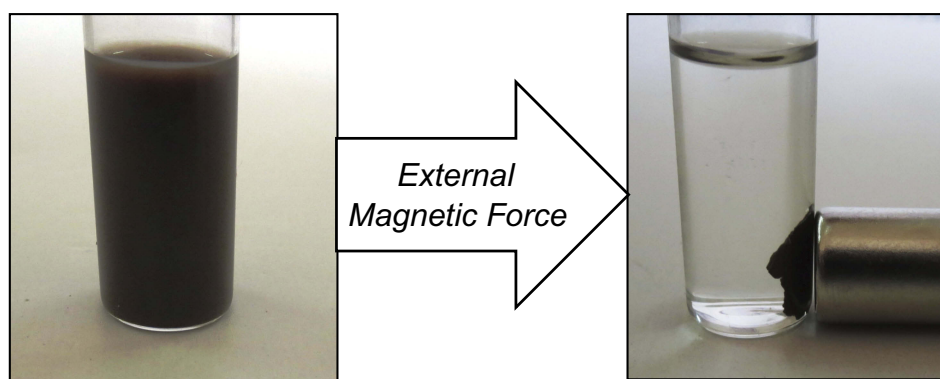


**Figure 7** Magnetic separation of enzyme-loaded polymer-grafted nanoparticles from the reaction mixture using a magnet.

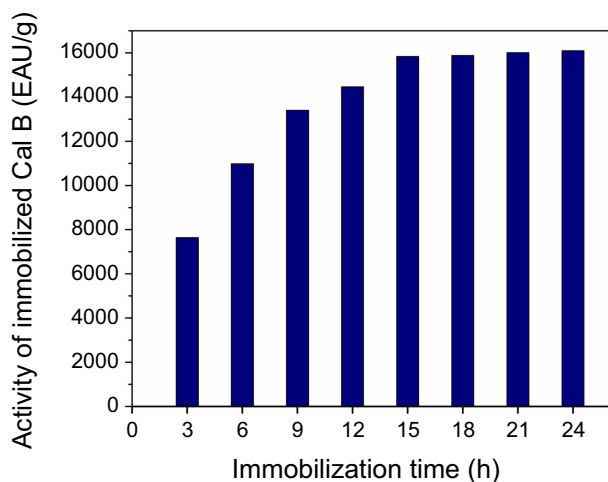


**Figure 8** Optimization of immobilization time for enzyme Cal-B on polymer-grafted magnetic silica nanoparticles.

**Table 1** Influence of enzyme Cal-B concentration on hydrolytic activity

S. No.	Loading <sup>a</sup> (EAU/g)	Amount of enzyme taken <sup>c</sup> (mL)	Lipase loaded (mg)	Hydrolytic activity (EAU/g)
1.	1,000	0.005	0.035	640
2.	5,000	0.025	0.175	3,920
3.	10,000	0.050	0.350	5,040
4.	15,000	0.075	0.525	8,000
5.	20,000	0.100	0.700	7,800
6.	25,000	0.125	0.875	7,640

**Notes:** <sup>a</sup>Cal-B immobilized by adsorption on polymer-grafted magnetic MNPs at pH 7 and room temperature. <sup>b</sup>50 mg of polymer-grafted MNPs were used as enzyme support. <sup>c</sup>Concentration of lipase solution used is 7 mg/mL.

MNPs showed improved enzymatic activity and favorable thermal and pH stability compared to the free enzyme, Cal-B. We also demonstrated that the enzyme-

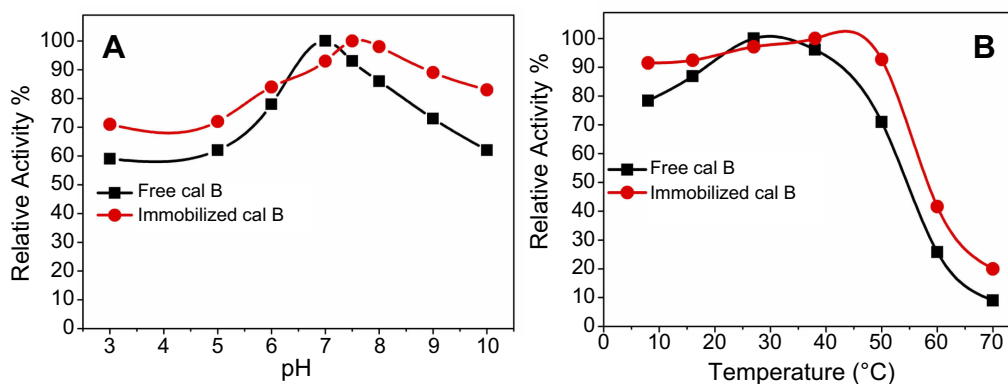


**Figure 9** Effect of (A) pH and (B) temperature on the activity of free and immobilized Cal-B enzyme.

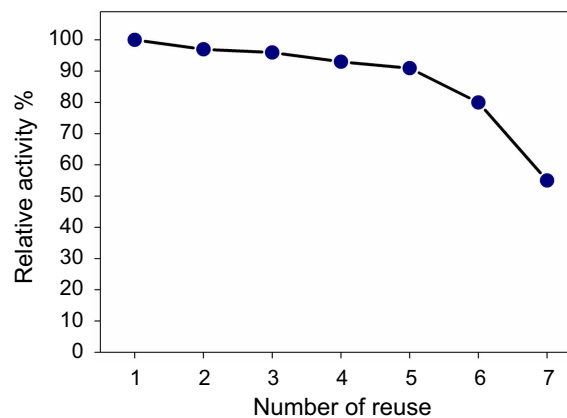


**Figure 10** Reusability of Cal-B enzyme-loaded polymer-grafted magnetic silica nanoparticles for hydrolytic activity.

immobilized MNPs showed good reusability and could be efficiently recovered magnetically. Overall, our work demonstrates that the immobilization of enzyme onto gallic acid resin-grafted magnetic iron oxide nanoparticles is efficient and cost-effective.

## Acknowledgments

This study was funded by Deanship of Scientific Research, King Faisal University, Al-Ahsa, Kingdom of Saudi Arabia. (Grant Number: 17122014). The authors thank Mr Tameem M Alyahian and Mr Naif Ali Alunssif (Laboratory Supervisor/Technician), College of Clinical Pharmacy King Faisal University for logistic support and handling instruments. The authors also thank Department of Science and Technology, India, for the support.

## Disclosure

The authors declare no conflicts of interest in this work.



## References

- Cen Y, Li D, Xu J, Wu Q, Wu Q, Lin X. Highly focused library-based engineering of *Candida antarctica* lipase B with (S)-selectivity towards sec-alcohols. *Adv Synth Catal.* 2019;361(1):126–134. doi:10.1002/adsc.201800711
- Gotor-Fernández V, Busto E, Gotor V. *Candida antarctica* lipase B: an ideal biocatalyst for the preparation of nitrogenated organic compounds. *Adv Synth Catal.* 2006;348(7-8):797–812. doi:10.1002/adsc.200606057
- Anderson EM, Larsson KM, Kirk O. One biocatalyst—many applications: the use of *Candida Antarctica* B-lipase in organic synthesis. *Biocatal Biotransform.* 1998;16(3):181–204. doi:10.3109/10242429809003198
- Secundo F, Carrea G. Lipase activity and conformation in neat organic solvents. *J Mol Catal B.* 2002;19–20:93–102. doi:10.1016/S1381-1177(02)00155-8
- Idris A, Bukhari A. Immobilized *Candida antarctica* lipase B: hydration, stripping off and application in ring opening polyester synthesis. *Biotechnol Adv.* 2012;30(3):550–563. doi:10.1016/j.biotechadv.2011.10.002
- Ghanem A. Trends in lipase-catalyzed asymmetric access to enantiomerically pure/enriched compounds. *Tetrahedron.* 2007;63(8):1721–1754. doi:10.1016/j.tet.2006.09.110
- Hasegawa S, Azuma M, Takahashi K. Enzymatic esterification of lactic acid, utilizing the basicity of particular polar organic solvents to suppress the acidity of lactic acid. *J Chem Technol Biotechnol.* 2008;83(11):1503–1510. doi:10.1002/jctb.v83:11
- Enzyme-catalyzed ring-opening polymerization of unsubstituted  $\beta$ -Lactam. *Macromol Rapid Commun.* 2008;29(10):794–797. doi:10.1002/marc.200800117
- Palomo JM, Muñoz G, Fernández-Lorente G, Mateo C, Fernández-Lafuente R, Guisan J. Interfacial adsorption of lipases on very hydrophobic support (octadecyl-Sepabeads): immobilization, hyperactivation and stabilization of the open form of lipases. 2002;19.
- Bornscheuer UT, Bessler C, Srinivas R, Krishna SH. Optimizing lipases and related enzymes for efficient application. *Trends Biotechnol.* 2002;20(10):433–437.
- Miletic N. *Improved Biocatalysts Based on Candida Antarctica Lipase B Immobilization.* 2009.
- Uppenberg J, Hansen MT, Patkar S, Jones TA. The sequence, crystal structure determination and refinement of two crystal forms of lipase B from *Candida antarctica*. *Structure.* 1994;2(4):293–308.
- Uppenberg J, Ohmer N, Norin M, et al. Crystallographic and molecular-modeling studies of lipase B from *Candida antarctica* reveal a stereospecificity pocket for secondary alcohols. *Biochemistry.* 1995;34(51):16838–16851.
- Kumar A, Dhar K, Kanwar SS, Arora PK. Lipase catalysis in organic solvents: advantages and applications. *Biol Proced Online.* 2016;18:2. doi:10.1186/s12575-016-0033-2
- Hlady V, Buijs J. Protein adsorption on solid surfaces. *Curr Opin Biotechnol.* 1996;7(1):72–77.
- Brigida AI, Pinheiro AD, Ferreira AL, Goncalves LR. Immobilization of *Candida antarctica* lipase B by adsorption to green coconut fiber. *Appl Biochem Biotechnol.* 2008;146(1–3):173–187. doi:10.1007/s12010-007-8072-4
- Miletic N, Vukovic Z, Nastasovic A, Loos K. Macroporous poly (glycidyl methacrylate-co-ethylene glycol dimethacrylate) resins—versatile immobilization supports for biocatalysts. *J Mol Catal B.* 2009;56(4):196–201. doi:10.1016/j.molcatb.2008.04.012
- Goradia D, Cooney J, Hodnett BK, Magner E. The adsorption characteristics, activity and stability of trypsin onto mesoporous silicates. *J Mol Catal B.* 2005;32(5):231–239. doi:10.1016/j.molcatb.2004.12.007
- Dumitriu E, Secundo F, Patarin J, Fechete I. Preparation and properties of lipase immobilized on MCM-36 support. *J Mol Catal B.* 2003;22(3):119–133. doi:10.1016/S1381-1177(03)00015-8
- Bai Y-X, Li Y-F, Yang Y, Yi L-X. Covalent immobilization of triacylglycerol lipase onto functionalized nanoscale SiO<sub>2</sub> spheres. *Process Biochem.* 2006;41(4):770–777. doi:10.1016/j.procbio.2005.09.012
- Kumar A, Gross RA, Jendrosseck D. Poly(3-hydroxybutyrate)-depolymerase from *Pseudomonas lemoignei*: catalysis of esterifications in organic media. *J Org Chem.* 2000;65(23):7800–7806.
- Mahapatro A, Kumar A, Kalra B, Gross RA. Solvent-free adipic acid/1,8-octanediol condensation polymerizations catalyzed by *Candida antarctica* lipase B. *Macromolecules.* 2004;37(1):35–40. doi:10.1021/ma025796w
- Hu J, Gao W, Kulshrestha A, Gross RA. “Sweet polyesters”: lipase-catalyzed condensation–polymerizations of alditols. *Macromolecules.* 2006;39(20):6789–6792. doi:10.1021/ma0612834
- Peeters J, Palmans ARA, Veld M, Scheijen F, Heise A, Meijer EW. Cascade synthesis of chiral block copolymers combining lipase catalyzed ring opening polymerization and atom transfer radical polymerization. *Biomacromolecules.* 2004;5(5):1862–1868. doi:10.1021/bm049794q
- Roach P, Farrar D, Perry CC. Interpretation of protein adsorption: surface-induced conformational changes. *J Am Chem Soc.* 2005;127(22):8168–8173. doi:10.1021/ja042898o
- Miletic N, Abetz V, Ebert K, Loos K. Immobilization of *Candida antarctica* lipase B on polystyrene nanoparticles. *Macromol Rapid Commun.* 2010;31(1):71–74. doi:10.1002/marc.200900497
- Dessouki AM, Atia KS. Immobilization of adenosine deaminase onto agarose and casein. *Biomacromolecules.* 2002;3(3):432–437.
- Duracher D, Elaïssari A, Mallet F, Pichot C. Adsorption of modified HIV-1 capsid p24 protein onto thermosensitive and cationic core–shell poly(styrene)–poly(N-isopropylacrylamide) particles. *Langmuir.* 2000;16(23):9002–9008. doi:10.1021/la0004045
- Fernández-Lorente G, Fernández-Lafuente R, Palomo JM, et al. Biocatalyst engineering exerts a dramatic effect on selectivity of hydrolysis catalyzed by immobilized lipases in aqueous medium. *J Mol Catal B.* 2001;11(4):649–656. doi:10.1016/S1381-1177(00)00080-1
- Mateo C, Palomo JM, Fernandez-Lorente G, Guisan JM, Fernandez-Lafuente R. Improvement of enzyme activity, stability and selectivity via immobilization techniques. *Enzyme Microb Technol.* 2007;40(6):1451–1463. doi:10.1016/j.enzmictec.2007.01.018
- Wilson L, Palomo JM, Fernández-Lorente G, Illanes A, Guisán JM, Fernández-Lafuente R. Improvement of the functional properties of a thermostable lipase from *Alcaligenes* sp. via strong adsorption on hydrophobic supports. *Enzyme Microb Technol.* 2006;38(7):975–980. doi:10.1016/j.enzmictec.2005.08.032
- Can M, Bulut E, Özacar M. Synthesis and characterization of gallic acid resin and its interaction with palladium(II), rhodium(III) chloro complexes. *Ind Eng Chem Res.* 2012;51(17):6052–6063. doi:10.1021/ie300437u
- Singh A, Mukhopadhyay M. Immobilization of *Candida antarctica* lipase onto cellulose acetate-coated Fe<sub>2</sub>O<sub>3</sub> nanoparticles for glycerolysis of olive oil. 2014;31.
- Lei L, Bai Y, Li Y, Yi L, Yang Y, Xia C. Study on immobilization of lipase onto magnetic microspheres with epoxy groups. *J Magn Magn Mater.* 2009;321(4):252–258. doi:10.1016/j.jmmm.2008.08.047
- Ding Y, Hu Y, Zhang L, Chen Y, Jiang X. Synthesis and magnetic properties of biocompatible hybrid hollow spheres. *Biomacromolecules.* 2006;7(6):1766–1772. doi:10.1021/bm060085h
- Liu X, Guan Y, Shen R, Liu H. Immobilization of lipase onto micron-size magnetic beads. *J Chromatogr B.* 2005;822(1):91–97. doi:10.1016/j.jchromb.2005.06.001

37. Dyal A, Loos K, Noto M, et al. Activity of *Candida rugosa* lipase immobilized on  $\gamma$ -Fe<sub>2</sub>O<sub>3</sub> magnetic nanoparticles. *J Am Chem Soc.* 2003;125(7):1684–1685. doi:10.1021/ja021223n
38. Ren Y, Rivera JG, He L, Kulkarni H, Lee D-K, Messersmith PB. Facile, high efficiency immobilization of lipase enzyme on magnetic iron oxide nanoparticles via a biomimetic coating. *BMC Biotechnol.* 2011;11(1):63. doi:10.1186/1472-6750-11-35
39. Stöber W, Fink A, Bohn E. Controlled growth of monodisperse silica spheres in the micron size range. *J Colloid Interface Sci.* 1968;26(1):62–69. doi:10.1016/0021-9797(68)90272-5
40. Lu AH, Salabas EL, Schuth F. Magnetic nanoparticles: synthesis, protection, functionalization, and application. *Angew Chem (Int Ed English).* 2007;46(8):1222–1244. doi:10.1002/anie.200602866
41. Woo E, Ponvel KM, Ahn I-S, Lee C-H. Synthesis of magnetic/silica nanoparticles with a core of magnetic clusters and their application for the immobilization of His-tagged enzymes. *J Mater Chem.* 2010;20(8):1511–1515. doi:10.1039/B918682D
42. Tie S-L, Lee H-C, Bae Y-S, Kim M-B, Lee K, Lee C-H. Monodisperse Fe<sub>3</sub>O<sub>4</sub>/Fe@SiO<sub>2</sub> core/shell nanoparticles with enhanced magnetic property. *Colloids Surf A.* 2007;293(1):278–285. doi:10.1016/j.colsurfa.2006.07.044
43. de Oliveira PC, Alves GM, de Castro HF. Immobilisation studies and catalytic properties of microbial lipase onto styrene–divinylbenzene copolymer. *Biochem Eng J.* 2000;5(1):63–71. doi:10.1016/S1369-703X(99)00061-3
44. Li C, Tan T, Zhang H, Feng W. Analysis of the conformational stability and activity of *Candida antarctica* lipase B in organic solvents: insight from molecular dynamics and quantum mechanics/simulations. *J Biol Chem.* 2010;285(37):28434–28441. doi:10.1074/jbc.M110.136200

### International Journal of Nanomedicine

Dovepress

### Publish your work in this journal

The International Journal of Nanomedicine is an international, peer-reviewed journal focusing on the application of nanotechnology in diagnostics, therapeutics, and drug delivery systems throughout the biomedical field. This journal is indexed on PubMed Central, MedLine, CAS, SciSearch®, Current Contents®/Clinical Medicine,

Journal Citation Reports/Science Edition, EMBase, Scopus and the Elsevier Bibliographic databases. The manuscript management system is completely online and includes a very quick and fair peer-review system, which is all easy to use. Visit <http://www.dovepress.com/testimonials.php> to read real quotes from published authors.

Submit your manuscript here: <https://www.dovepress.com/international-journal-of-nanomedicine-journal>